IOSR Journal of Mechanical and Civil Engineering (IOSR-JMCE)
e-ISSN: 2278-1684,p-ISSN: 2320-334X, Volume 14, Issue 6 Ver. II (Nov. - Dec. 2017), PP 47-54
www.iosrjournals.org

Mechatronic Modelling of A Wind Turbine Gear Box Based on Bond Graph

Zakaria Khaouch[1], Youssef Najih[1], Mustapha Adar[1],Mustapha Zekraoui[1], Nourreeddine Kouider[1], Mustapha Mabrouki[1]

[1]*Industrial Engineering Laboratory, Faculty of Science and Technology, Sultan Moulay Slimane University, Beni Mellal, Morocco.*

Corresponding Author: Zakaria Khaouch1

Abstract: *In this paper, a wind turbine gearbox model, which is realized through a Bond Graph Approach, is presented to analyze the dynamic behavior of a wind turbine transmission. In this regard, the wind turbines gearbox consists of three stages. The first one is a planetary gear and the two others are parallel gears. Taking account of meshing and torsional stiffness and dumping, the dynamic model of each stage is established. Consequently, the whole model is integrated following the Bond Graph modeling procedure. Subsequently, vibration analysis of the gearbox is carried out to demonstrate the application of the Bond Graph model in mode analysis. Finally, the dynamic characteristics of a wind turbine gearbox using the proposed model are analyzed and verified based on 20-sim program.*

Keywords: *Bond graph, Gearbox, Mechatronic modelling, Wind turbine.*

Date of Submission: 14 -10-2017 Date of acceptance: 30-11-2017

I. Introduction

The power generation with wind turbines has grown during the past twenty years. The customers who are environmentally conscious have now been using this clean wind energy from power providers. The global market for the electrical power produced by wind turbine generator has been increasing steadily, which directly pushes the wind power technology into a more competitive area [1-6]. The wind turbine system is composed of rotor, gearbox, generator, AC/DC/AC converter and grid. The power from the rotation of the wind turbine rotor is transferred to the generator through the power train, i.e. through the main shaft, the gearbox and the high speed shaft. The gearbox is typically used in a wind turbine to increase rotational speed from a low-speed rotor to a higher speed electrical generator. It is the most important part of a wind turbine, where most of faults occur. In [7] it is reported that a wind turbine has around 20 years of life span, but normally the gearbox needs to be replaced every 5 years. For this reason, big manufacturing companies of wind turbines intend to use a direct drive wind turbine without a gearbox.

Nowadays, most of the installed wind turbines are equipped with a gearbox specially the planetary gears because of their compact design and high efficiency [8,9]. Actually, most of the 270 GW of wind turbine power is installed around the world with this configuration [10,11]. Based on this context, a model of the gearbox is presented in this paper. In terms of a Bond Graph Approach, The modeling of a gearbox has been addressed in several works. [12] Observed chaos in the dynamic response of a geared rotor-bearing system with bearing clearance and backlash. [13] Studied the effects of backlash and bearing clearance in a geared flexible rotor and the interactions between these two nonlinearities. [14] Investigated the nonlinear effects and instability caused by bearing clearance in helicopter planetary gears. [15,16] Studied the dynamics of a mechanical oscillator with clearance nonlinearity and fluctuating mesh stiffness, and correlated results with experimental data. [17,18] investigated primary resonances, subharmonic resonances, and chaos in a multimesh gear train caused by fluctuating gear mesh stiffness. [19,20] Studied the dynamics of wind turbine planetary gears with gravity effects using an extended harmonic balance method that includes simultaneous internal and external excitations. The Bond Graph model of a gearbox has been addressed in a few works [22, 23]. In this present work, a Bond Graph model of wind turbine gearbox is presented, all gear component are modeled id detail, taking into account its dynamic behavior.

II. Fundamental Concepts Of Bond Graphs

A Bond Graph [24,25,26,27] is a graphical way of modeling physical systems. All these physical systems have in common the conservation laws for mass and energy. Bond graph, originated by Paynter in 1961, deals with the conservation of energy. This gives a unified approach to modeling physical systems. Further follows a short introduction to this modeling tool, more information can be found in. The bond graph based modelling has several advantages over conventional simulation methods as follows:

1. Providing a visual representation of the design;
2. Controlling the consistency of the topological settings of the design;
3. Providing the hierarchical modelling of designs;
4. Extracting the system equations symbolically in a structured way.

Within physical systems, energy is transported form one item to another. This energy is either stored or converted to other forms. However, the important thing is that it does not dissipate. If the energy is changing in one place, it also changes in an opposite way at another location. The definition of power P is the change in energy E with respect to time:

$$P = \frac{dE}{Dt} \qquad 1)$$

This power is transferred between the different parts in bond graph model with the use of power bonds, see Fig. 1. Power can be expressed as the product of an effort and a flow variable, thus the general expression:

$$P = e(t)f(t) \qquad (2)$$

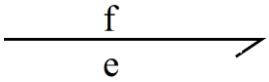

Fig. 1 Power bond with effort and flow

The symbols e(t) and f(t) are used to denote effect and flow quantities as functions of time. Table 1 shows what the effort and flow quantities can be in some familiar domains.

Table 1: Effort and flow variables in different domains

Domain	Effort, e(t)	Flow, f(t)
Mechanical translation	Force, F(t)	Velocity, v(t)
Mechanicalrotation	Toque, τ(t)	Angularvelocity, ω(t)
Hydrolic	Pressure, P(t)	Volume flow rate, Q(t)
Electric	Voltage, U(t)	Current, i(t)

2.1. System Elements

In bond graph modeling there are a total amount of nine different elements. We will also here introduce the causality assignments, but first we have to explore the cause and effect for each of the basic bond graph elements.

2.1.1. Junctions:

There are two different types of junctions that connects the different parts in a bond graph model. The 0-junction and the 1-junction. The 0-junction is an effort equalizing connection, see Fig. 2 and its corresponding equations in (3). Since the efforts are the same, only one bond can decide what it is. The 1-junction is a flow equalizing connection, see Fig. 3 and its corresponding equations in (4). Since the flows are the same, only one bond can decide what it is. Which bond decides the flow and which one decides the effort is indicated with the vertical causality stroke. If the vertical line is closest to the junction, then this element decides the effort, furthest away from the junction decides the flow.

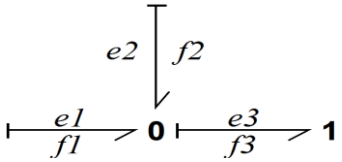

Fig. 2 0-junction

$$\begin{cases} e_1 = e_2 = e_3 \\ f_3 = f_1 + f_2 \end{cases} \quad 3)$$

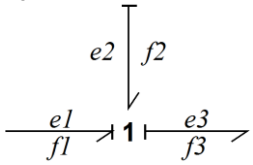

Fig. 3 1-junction

$$\begin{cases} f_1 = f_2 = f_3 \\ e_3 = e_1 + e_2 \end{cases} \quad (4)$$

2.1.2. Source Element

We can divide the source elements into two different kinds, effort- and flow-source. The effort source gives an effort into the system, and then it is up to the system to decide the flow. This is what is meant with cause and effect, and its vice versa for the flow source. Fig. 4 shows how the causality is indicated on the graphical elements. For the source elements these causality assignments are fixed.

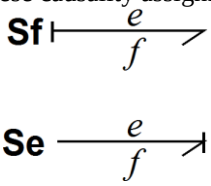

Fig. 4 Effort and flow source with their causality assignment

2.1.3. Compliance Element

The causality assignment for the C-element has two possibilities, but one is preferred in contrast to the other. This is discussed at the end of this section. The preferred case is seen in Fig.5 and its corresponding equation in (5). We see from both the equation and the figure that flow is given to the element/equation and it gives the effort in return.

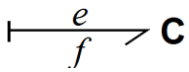

Fig. 5 Example of a compliance element with integral causality

$$e = \frac{1}{C}\int f dt = \frac{q}{C} \quad 5)$$

The variable *q*is called the generalized displacement. For example, this can be rotational position of the rotor in a wind turbine.

2.1.4. InertiaElement

There are two choices for the causality assignment for the I-element, also here one is preferred in contrast to other. The preferred case is seen in Fig. 6 and its corresponding equation in (6).

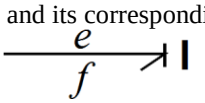

Fig. 6 Example of an inertia element with integral causality

$$f = \frac{1}{I}e = \frac{p}{I} \quad 6)$$

The variable p is called the generalized momentum. For example, this can be rotor inertia times rotor velocity in a wind turbine.

2.1.5. ResistiveElement

It is a bit more freedom when it comes to the causality assignment for the R-element. Its equation do not include any dynamics, it is only an algebraic expression. The two causality choices are shown in Fig. 7 and its corresponding equation in (7).

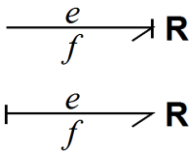

Fig. 7 Example of resistive element

$$f = \frac{e}{R} \quad \text{or} \quad e = Rf \tag{7}$$

2.1.6. Transformer Element

The transformer element can work in two ways; either it transforms a flow into another flow or it transforms an effort into another effort. Fig. 8 corresponds to (8), where m is the transformation ratio. For example, this can represent a mechanical gearing or an electric transformer.

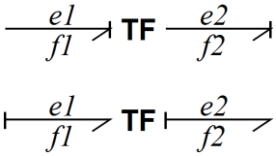

Fig. 8 Example of the two transformers

$$f_1 = \frac{f_2}{m}, \quad e_2 = \frac{e_1}{m} \quad \text{or} \quad f_2 = mf_1, \quad e_1 = me_2 \tag{8}$$

2.1.7. GyratorElement

The gyrator can also work in two ways; either it transform a flow into an effort or it transform an effort into a flow. Fig. 9 corresponds to (9), where r is the gyrator ratio.

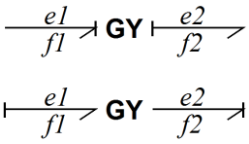

Fig.9 Example of the two gyrators

$$f_1 = \frac{e_2}{r}, \quad f_2 = \frac{e_1}{r} \quad \text{or} \quad e_1 = rf_2, \quad e_2 = rf_1 \tag{9}$$

By using bond graph as the modeling tool we get a good overview of the models physical structure and we can do simulations in one step, instead of first deriving the equations and then drawing the block diagram.

III. Bond Graph Model of the Wind Turbine Gearbox.

Wind turbines gearbox presented in this paper is consists of three stages. The first one is a planetary gear and the two others are parallel gears. The gearbox scheme is shown in Fig. 10.

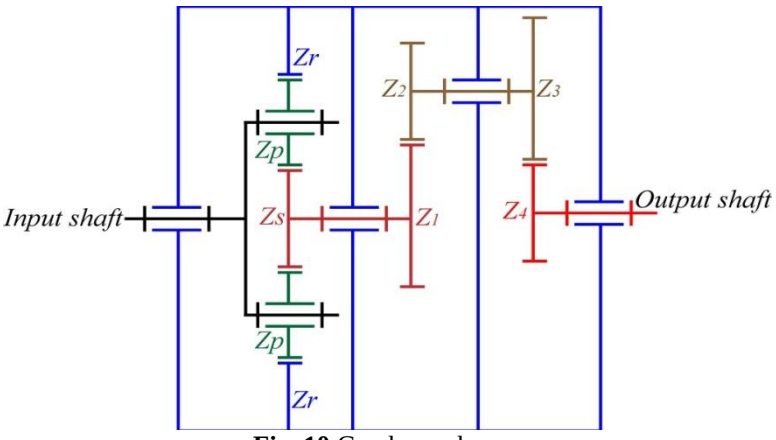

Fig. 10 Gearbox scheme

The gearbox can be considered as a simple model in which the conversion ratio can be introduced directly in a transformer (TF-element of Bond Graph). However this model does not describe the dynamic behavior of the gearbox. Therefore, a more accurate model needs to be developed. This model will be used in a future work as a base, in order to formulate the law control to compensate any perturbation due to a gearbox default.

In [28] a detailed gearbox Bond Graph model is proposed. The planetary gear model is presented in detail but the parallel stage is modeled by a simple *TF* element. This resource is taken as a reference to develop the wind turbine gearbox model, to which we add a detailed model of parallel gear stage. Moreover, the dampers of all components of the system are also considered. For a planetary gear, several identical planet (*p*) gears are in mesh with the sun gear and the ring gear (*r*), and the carrier (*c*) holds all of the planet gears. Planet gears rotate in two kinematic modes called revolution around the sun gear and autorotation around its own axis. Power flow into the planetary gear will split or converge. A basic kinematic model of a single planetary gear is shown in Fig. 11.

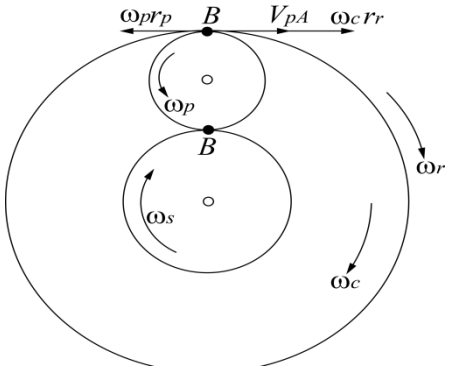

Fig. 11 Kinematic model of planetary gearbox

According to the kinematic relation of the components shown in Fig. 21, the translation velocities in contact point A and B can be described as follows:

$$V_{pA} = -\omega_p r_p + \omega_c r_r \quad (20)$$

$$V_{rA} = \omega_r r_r \quad (21)$$

$$V_{pB} = \omega_p r_p + \omega_c r_s \quad (22)$$

$$V_{sB} = \omega_s r_s \quad (23)$$

where, ω_j and r_j stand for the rotating velocity and the base circle radius ($j = r,s,p$) respectively. A is the meshing point of the ring gear and the planet, and B is the meshing point of the sun gear and the planet. V_{pm} is the velocity of planets in point m along tangent direction, where $m = A,B$. Similarly, V_{rA} and V_{sB} are the linear velocities of ring gear in *A* and sun gear in *B*. In a gear systems modeling, the gear mesh interfaces are usually consideredas spring-damper systems [27]. The spring stiffness (also called the mesh stiffness), is one of the major sources of gear vibration. The dynamic model of planetary gearbox is shown in Fig. 11(a). Fig. 11(b) depicts the Bond Graph model of the gearbox.

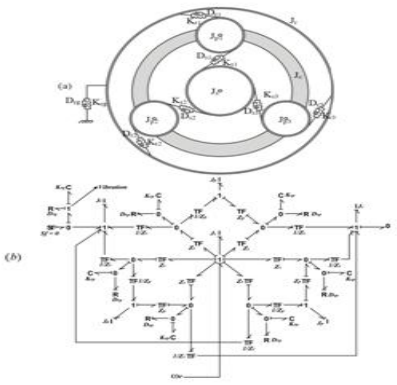

Fig. 11 Physical model for dynamic meshing problem (a), bond graph model of planetary gearbox (b)

The planet gears represented by momentum of inertia $J_{pi}$are connected to each other through a common carrier. Therefore, they get the same rotational speed imposed by the carrier. 1-junction represents the rotation speed of the carrier (*c*), and I−elements J_c denote the rotary inertia of the carrier. These planets are bounded to sun and ring gears by the mesh stiffness dumping K_{sp},B_{sp} and K_{rp},B_{rp} respectively. J_r is the ring gears momentum of inertia. The connection between the ring and the hub is carried out by an elastic joint modeled through a spring-damper. In this joint, the vibration signal of the gear can be obtained. In the model, *Zi,(i = p,s,r)* represents the teeth number of each gear. The flow 1-junction represents the angular velocity of planets, carrier, ring and sun gear, respectively. They are related to each other through TF-elements.

The zero junctions, between the transformers, represent the effort variable that the planet moves in tangential direction. The parallel gear stage of the wind turbine gearbox is composed of two stages. The dynamic model and the bond graph model are shown in Fig 12.

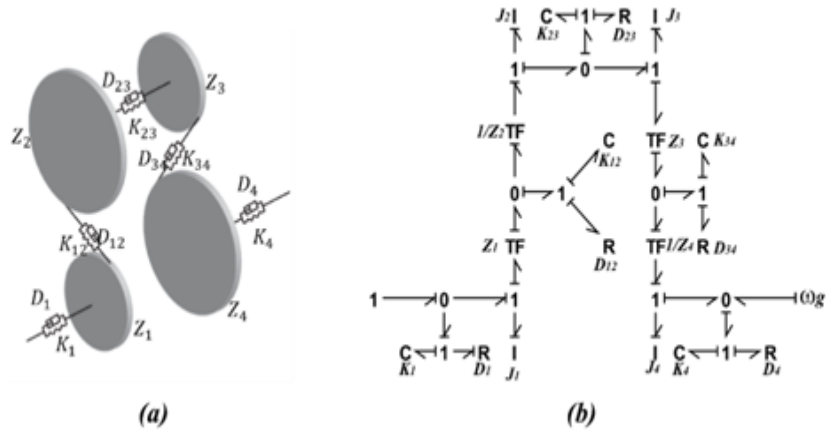

Fig. 12 Dynamic model of parallel gear (a), Bond graph model of parallel gear(b)

The complete Bond Graph model of a wind turbine gearbox and its sub-models are depicted in Fig. 13.

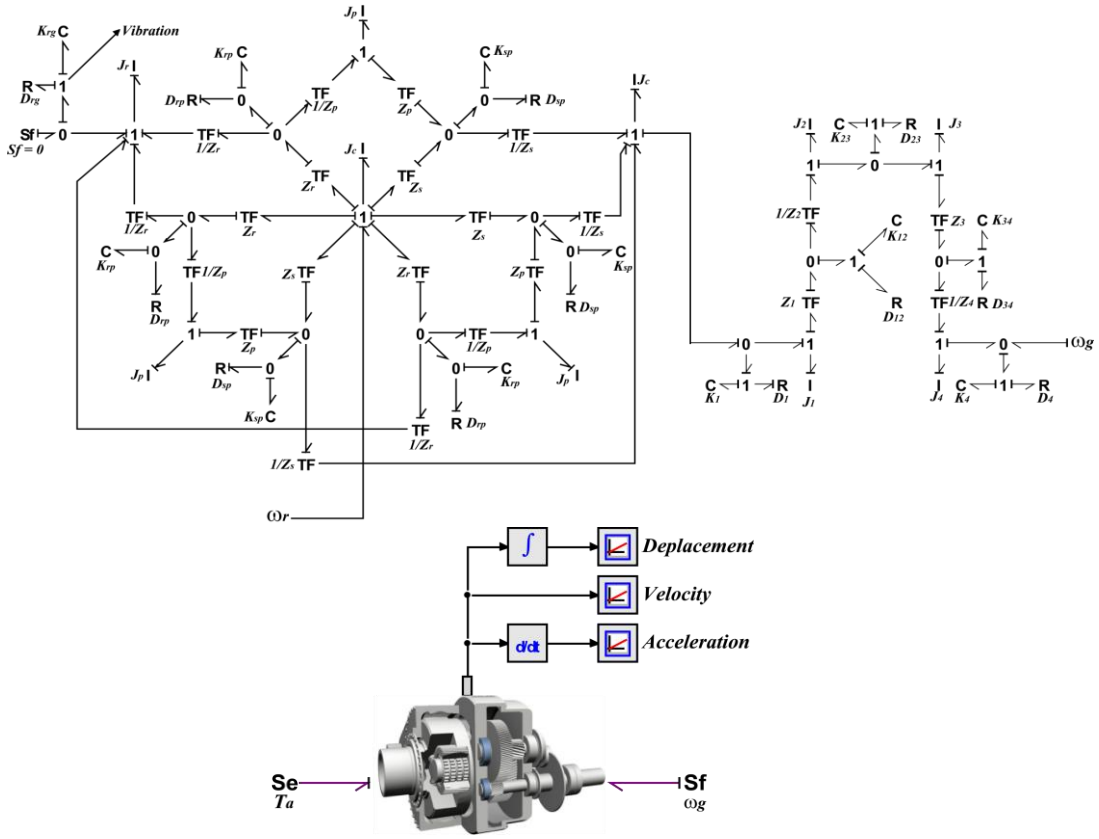

Fig. 13 Bond graph model and sub-model of a wind turbine gearbox

IV. Simulation And Results

Fig. 14 represents a simulation of the gearbox behaviors. A constant torque is applied at the input of the gearbox (Se = 60N.m). This output torque decreases with a ratio of 60. The same outcome is observed in the angular velocity curves. For a constant angular velocity at the gearbox output, the gearbox input is reduced with a ratio of 60. From the teeth number of each gear (Appendix A), we can calculate the gearbox ratio, which is equal to 60. Thiscomes in line with the predictions of the gears bond graph model. The system undergoes the same vibrations patterns; which are due to the dynamics involved between the mesh stiffness and the momentum of inertias.

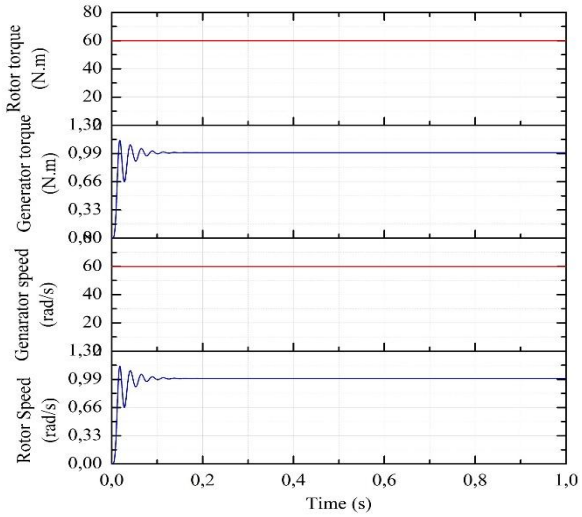

Fig. 14 Gearbox simulation model

V. Conclusions

A generalized dynamic model of the wind turbine gearbox– witch composed of three stages (one stages is a planet gear and the two other stages are parallel gears) – considered the meshing stiffness and damping based onBond Graph theory is set up. All gearbox components are modeled in detail and all dynamic behavers are takings into consideration,a good results are obtained by simulation. This model will be used in a future work as a base for vibration analysis and to calculate the natural frequencies and the displacement mode shapes, the model can be used to develop law control in order to compensate any perturbation due to a gearbox default.

References

[1]. E. Hau, WindkraftanlagenGrundlagen, Technik, Einsatz, Wirtschaftlichkeit, Springer, 1996.
[2]. Wind in power, European Statistics, the European Energy Association, Feb.2015, 2014.
[3]. Soren Krohn, Poul-Erik Morthorst, Shimon Awerbuch. The economics of wind energy. The European Wind Energy Association; 2009.
[4]. Jacobson Mark Z, Delucchi Mark A, Ingraffea Anthony R, Howarth Robert W, Bazouin Guillaume, Bridgeland Brett, et al. A roadmap for repowering California for all purposes with wind, water, and sunlight. Energy 2014;73: 875e89.
[5]. Oh Ki-Yong, Kim Ji-Young, Lee Jun-Shin, Ryu Ki-Wahn. Wind resource assessment around Korean Peninsula for feasibility study on 100 MW class offshore wind farm. Renew Energy 2012;42:217e26.
[6]. Oh Ki-Yong, Kim Ji-Young, Lee Jae-Kyung, Ryu Moo-Sung, Lee Jun-Shin. An assessment of wind energy potential at the demonstration offshore wind farm in Korea. Energy 2012;46:555e63.
[7]. S. Agarwal, L. Chalal, G. Dauphin-Tanguy, X. Guillaud, Bond Graph Model of Wind Turbine Blade, Bond Graph Modeling: Theory and Practice MathMod Vienna, 2012.
[8]. Y. Guo and R. G. Parker, "Dynamic modeling and analysis of a spur planetary gear involving tooth wedging and bearing clearance nonlinearity," European Journal of Mechanics A/Solids, vol. 29, pp. 1022-1033, 2010.
[9]. Yi Guo, Jonathan Keller, Robert G. Parker. Dynamic Analysis of Wind Turbine Planetary Gears Using an Extended Harmonic Balance Approach International Conference on Noise and Vibration Engineering Leuven, Belgium September 17-19, 2012.
[10]. Christopher J. Spruce and Judith K. Turner, Tower Vibration Control of Active Stall Wind Turbines, JULY 2013.
[11]. GWEC, Global Wind Statistics 2012, Global Wind Energy Council, February 2013.
[12]. A. Kahraman and R. Singh, "Nonlinear dynamics of a geared rotor-bearing system with multiple clearances," Journal of Sound and Vibration, vol. 144, pp. 469-506, 1991.
[13]. N. E. Gurkan and H. Ozguven, "Interactions between backlash and bearing clearance nonlinearity in geared flexible rotors," in ASME International Design Engineering Technical Conferences and Computers and Information in Engineering Conference, 2007.
[14]. Y. Guo and R. G. Parker, "Dynamics of planetary gears with bearing clearance," ASME Jounal of Computational Nonlinear Dynamics, vol. 7, no. 3, p. 031008, 2012.
[15]. G. W. Blankenship and A. Kahraman, "Steady state forced response of a mechanical oscillator with combined parametric excitation and clearance type non-linearity," Journal of Sound and Vibration, vol. 185, no. 5, pp. 743-765, 1995.
[16]. A. Kahraman and G. W. Blankenship, "Experiments on nonlinear dynamic behavior of an oscillator with clearance and periodically time-varying parameters," Journal of Applied Mechanics, vol. 64, pp. 217-226, 1997.

[17]. A. Al-shyyab and A. Kahraman, "Non-linear dynamic analysis of a multi-mesh gear train using multi-term harmonic balance method: period-one motions," Journal of Sound and Vibration, vol. 284, no. 1-2, pp. 151-172, 2005.
[18]. A. Al-shyyab and A. Kahraman, "Non-linear dynamic analysis of a multi-mesh gear train using multi-term harmonic balance method: subharmonic motions," Journal of Sound and Vibration, vol. 279, no. 1-2, pp. 417-451, 2005.
[19]. Y. Guo and R. G. Parker, "Dynamic modeling and analysis of a spur planetary gear involving tooth wedging and bearing clearance nonlinearity," European Journal of Mechanics A/Solids, vol. 29, pp. 1022-1033, 2010.
[20]. Yi Guo, Jonathan Keller, Robert G. Parker. Dynamic Analysis of Wind Turbine Planetary Gears Using an Extended Harmonic Balance Approach International Conference on Noise and Vibration Engineering Leuven, Belgium September 17-19, 2012.
[21]. N. Coudert, G. Dauphin-Tanguy, A. Rault, Mechatronic Design of an Automatic Gear Box using Bond Graphs, in: Proceedings of the IEEE Systems Man and Cybernetics Conference, 1993.
[22]. Deur Joko, Ivanovic Vladimir, Assadian Francis, Kuang Ming, H. Tseng Eric, Hrovat, Bond graph modeling of automotive transmissions and drivelines, in: Proceedings of 7th Vienna International Conference on Mathematical Modelling (MATHMOD), Vienna, Austria, 2012.
[23]. Zakaria Khaouch, Mustapha Zekraoui, JamaaBengourram, Nourreeddine Kouider, Mustapha Mabrouki. Mechatronic modeling of a 750 kW fixed-speed wind energy conversion system using the Bond Graph Approach. ISA Transactions 65 (2016) 418436.
[24]. Zakaria Khaouch, Mustapha Zekraoui, Nourreeddine Kouider, Mustapha Mabrouki, JamaaBengourram. Mechatronic Modeling and Control of a Nonlinear Variable-Speed Variable-Pitch Wind Turbine by Using the Bond Graph Approach. IOSR Journal of Electrical and Electronics Engineering (IOSR-JEEE). e-ISSN: 2278-1676,p-ISSN: 2320-3331, Volume 11, Issue 6 Ver. I (Nov. - Dec. 2016), PP 95-115
[25]. Margolis Donald. Bond Graph Modelling of Engineering Systems: Theory, Applications and Software Support; 2011.
[26]. MerzoukiRochdi, SamantarayArun Kumar, Pathak Pushparaj Mani, OuldBouamamaBelkacem. Intelligent mechatronic systems: modeling, control and diagnosis. 2013.
[27]. R. Sanchez, A. Medina. Wind turbine model simulation: A bond graph approach. Simulation Modelling Practice and Theory. 2014;41:28-45.

Zakaria Khaouch" Mechatronic Modelling of A Wind Turbine Gear Box Based on Bond Graph.” IOSR Journal of Mechanical and Civil Engineering (IOSR-JMCE) , vol. 14, no. 6, 2017, pp. 47-54.